

# General CAV platoon considering the time-varying communication delay: system modeling and stability

Tiancheng Ruan, Hao Wang, Xiaopeng Li, Gengyue Han, Beier Ba, Changyin Dong,

**Abstract**—Driven by the potential of connected autonomous vehicles (CAVs), recent research has focused on their potential benefits in terms of safety, emissions, and capability. However, achieving these benefits is preconditioned on ensuring stability, which is the primary goal of CAVs. Despite the widespread adoption of feedback control to achieve stability, it cannot be guaranteed absolutely due to the communication delay that is inherent in CAVs. To address this issue, a considerable amount of research has been conducted to derive stability conditions considering communication delay. However, most of the research has implicitly assumed that the communication delay is constant, representing the maximum communication delay, which does not reflect the reality that the communication delay is time-varying based on the surrounding environment. Therefore, this paper proposes a generic supermatrix modeling approach for the CAV platoon that considers time-varying communication delay. Additionally, a novel stability condition is derived considering the time-varying delay of the generic CAV platoon, using the Lyapunov-Krasovskii Stability Theorem and Wirtinger-Based Integral Inequality. Furthermore, extensive numerical analyses are conducted in various scenarios to evaluate the tracking performance and safety conditions of different control parameters and information flow topologies (IFTs). The results indicate that all CAVs have smooth tracking performance if stability is guaranteed. Increasing the gain of spacing and velocity errors can benefit tracking performance and safety conditions, while increasing the gain of acceleration errors does not. Moreover, leader-based and bi-directional communication enable superior tracking and transient performance.

**Index Terms**—Connected and Automated Vehicles (CAVs); Time-varying communication delay; CAV platoon; Stability analysis; Tracking performance.

## I. INTRODUCTION

AUTOMOTIVE engineers have been tirelessly committed to enhancing the safety and comfort of automobile travel since its inception over a century ago. However, traffic problems such as traffic congestion, accidents, and pollutant emissions have become more prominent in recent decades [1, 2, 3]. Traditional traffic engineers have implemented external measures such as traffic management and traffic control to address these issues. However, these measures are becoming increasingly ineffective and are encountering bottlenecks.

T. Ruan, H. Wang, G. Han, B. Ba and C. Dong are with the School of Transportation, Southeast University, Nanjing 211189, P.R. China; Jiangsu Key Laboratory of Urban ITS, Southeast University, Nanjing, 210096, P.R. China; Jiangsu Province Collaborative Innovation Center of Modern Urban Traffic Technologies, Southeast University, Nanjing, 210096, P.R. China(e-mail: ruantiancheng@seu.edu.cn; haowang@seu.edu.cn; gyhan@seu.edu.cn; 980794728@qq.com; dongcy@seu.edu.cn).

Xiaopeng. Li is with Department of Civil & Environmental Engineering, University of Wisconsin-Madison, Madison, 53706, USA(e-mail: xli2485@wisc.edu).

Manuscript received March 2, 2023.(Corresponding author: Hao Wang.)

Research on the static and dynamic characteristics of traffic flow has identified the heterogeneity of human factors as the primary cause of this phenomenon [4, 5, 6, 7].

Automated Vehicles (AVs) have emerged as a promising enabler, benefiting from advancements in technology, and have made significant strides in both the automotive industry and academia in recent years. AVs measure the state error relative to their predecessors through on-board sensing devices, enabling precise tracking. Due to their simplicity and effectiveness, AVs are increasingly regarded as a standard device for modern commercial vehicles, and their market penetration rate (MPR) is growing [8, 9]. Consequently, much research on AVs has revealed their superiority over human-operated vehicles in terms of capacity, safety, and emissions [10, 11, 12].

However, AVs are restricted by limited access to information and, therefore, cannot fully utilize the potential of autonomous driving. Thanks to the advancement of wireless communication technology and Cellular Vehicle-to-Everything (C-V2X), Connected Automated Vehicles (CAVs) have emerged. Equipped with Vehicle-to-Infrastructure (V2I) and Vehicle-to-Vehicle (V2V) communication, CAVs can acquire information more accurately and with less delay, even beyond the sight [13, 14]. Moreover, CAVs have the potential to implement more elaborate platoon control strategies compared to AVs [15, 16], enabling the CAV platoon to achieve system optimization rather than user optimization to leverage further the safety and capacity gains of CAVs [17, 18]. Currently, extensive research has been conducted on CAVs, including the exploration of their capacity gains [19, 20], safety improvement [21, 22, 23], and reduction of pollutant emissions [24, 25].

Despite the advantages mentioned above of CAVs, their stability is the primary goal, and a prerequisite for utilizing these benefits. Specifically, transient response caused by perturbation fades with time. However, due to unavoidable communication delay, stability cannot be absolutely guaranteed by widely adopted feedback control. Therefore, extensive research has been conducted to derive stability conditions considering delay [26, 27, 28, 29, 30, 31].

In early research, Herman et al. [26] adopted a Laplace transform-based approach to a simple linear time-delay model and derived its characteristic equations. Then the stability conditions were obtained through numerical methods. Zhang and Jarrett [27] further developed this approach by considering the product of sensitivity and reaction time in a linear time-delay model. They obtained a more general and analytic stability condition through a characteristic equation-based approach. Li et al. [28, 29] used the full velocity difference car-following

model to derive a stability condition using the second Lyapunov method and conducted simulations to evaluate the effect of different parameters on the dynamic performance. Kamath et al. [30] linearized the optimal velocity model and the classical car-following model to construct the characteristic equation considering reaction delay, and then used the Nyquist stability criterion to derive the corresponding stability conditions. Then, Sun et al. [31] provided a comprehensive review of these methods and verified the consistency and applicability of some stability conditions through numerical simulations.

Although the above stability analysis methods can effectively derive stability conditions considering communication delay, most assume a constant delay that represents the maximum communication delay, limited by the fundamental methodology adopted. However, in practice, the communication delay is time-varying, depending on the surrounding environment's variation. This is because the basic methodology of the aforementioned methods can be divided mainly into methods based on the frequency domain and methods based on the second Lyapunov method. The high dimensionality in time-varying time-delay systems makes it challenging to apply frequency domain-based methods as the time-varying delay converts the problem into an analytically difficult infinite-dimensional one, represented by a delay-differential equation [32]. Second Lyapunov method-based methods need to be generalized to the functional space when dealing with time-varying time delays, leading to additional constraints for different trajectories. This leads to conservativeness of the obtained stability conditions due to approximations and additional constraints [33, 34, 35]. Therefore, a stability analysis method capable of handling time-varying delay needs to be developed to obtain more accurate stability conditions.

Thus, in this paper, a generic supermatrix modeling approach is proposed for the CAV platoon considering the time-varying communication delay. Moreover, a novel stability condition is derived for the generic CAV platoon considering the time-varying delay by applying the Wirtinger-Based Integral Inequality and Lyapunov-Krasovskii Stability Theorem. To sum up, the main contributions of this paper can be divided into four aspects:

- 1) A generic supermatrix modeling approach is proposed for the CAV platoon considering time-varying communication delay.
- 2) A novel stability condition is derived for the CAV platoon considering the time-varying delay under the general representation based on the Lyapunov-Krasovskii Stability Theorem.
- 3) The Wirtinger-Based Integral Inequality is adopted instead of the Jensen inequality to obtain a more accurate stability condition.
- 4) Extensive numerical analyses are conducted in various scenarios to comprehensively evaluate the tracking performance and safety conditions of different control parameters and provide guidance for their selection.

The remainder of the paper is outlined as follows: Section II provides an introduction to the mathematical preliminaries, including graph theory and two essential integral inequalities.

In Section III, the proposed supermatrix modeling approach of the CAV platoon, considering time-varying communication delay and a corresponding general representation, is presented. Corresponding stability analyses and the derivation of stability conditions are conducted in Section IV. Section V comprehensively evaluates the tracking performance and safety conditions of different control parameters through a performance evaluation analysis. Finally, the paper is summarized in Section VI.

## II. PRELIMINARIES

**Notations:** Throughout the paper  $\mathbb{R}^n$  denotes the n-dimensional Euclidean space with Euclidian norm  $|\cdot|$  while the set of all  $m \times n$  real matrices is denoted by  $\mathbb{R}^{m \times n}$ . The sets  $\mathbb{S}_n$  means the set of symmetric matrices of  $\mathbb{R}^{n \times n}$  while  $\mathbb{S}_n^+$  denotes the set of symmetric positive definite matrices. Moreover,  $p_i(t)$ ,  $v_i(t) = \dot{p}_i(t)$ ,  $a_i(t) = \ddot{p}_i(t)$ , and  $\dot{a}_i(t) = \dddot{p}_i(t) \in \mathbb{R}$  denote the longitudinal position, speed, acceleration, and jerk of vehicle  $i$  at time  $t$ , respectively. The transpose of a vector or a matrix  $A$  is denoted by  $A^T$ . The symmetric matrix  $\begin{bmatrix} A & B \\ * & C \end{bmatrix}$

denotes  $\begin{bmatrix} A & B \\ B^T & C \end{bmatrix}$ . Besides,  $He(K)$  represents  $K + K^T$  for any square matrix  $K \in \mathbb{R}^{n \times n}$ .  $I_n$  defines the identity matrix of  $n \times n$  while  $0_{m,n}$  denotes the zero matrix of  $m \times n$  dimension. For any matrix  $A \in \mathbb{R}^{n \times n}$ ,  $A > 0$  denotes that  $A$  is symmetric and positive definite. The Banach space  $C([-h, 0], \mathbb{R}^n)$  is used to denote the set of continuous functions from the interval  $[-h, 0] \subset \mathbb{R}$  to  $\mathbb{R}^n$  that are also square integrable. For any function  $f \in C$ , the uniform norm  $|f|_h$  refers to  $\sup_{\theta \in [-h, 0]} |f(\theta)|$ .  $diag\{a_1, a_2, \dots, a_n\}$

stands for the diagonal matrix  $\begin{bmatrix} a_1 & 0 & 0 \\ 0 & \ddots & 0 \\ 0 & 0 & a_n \end{bmatrix}$  whose diagonal elements from the top left corner are  $a_1, a_2, \dots, a_n$ .

Let  $A \in \mathbb{R}^{m \times n}$  and  $B \in \mathbb{R}^{p \times q}$ . The Kronecker product of  $A$  and  $B$  is denoted as  $A \otimes B$  and defined as follows:

$$A \otimes B = \begin{bmatrix} a_{11}B & \cdots & a_{1n}B \\ \vdots & \ddots & \vdots \\ a_{m1}B & \cdots & a_{mn}B \end{bmatrix} \in \mathbb{R}^{mp \times nq}.$$

Let  $C \in \mathbb{R}^{m \times n}$  and  $D \in \mathbb{R}^{n \times n}$ . The Hadamard product of  $C$  and  $D$  is denoted as  $C \circ D$  and defined as follows:

$$C \circ D = \begin{bmatrix} c_{11}d_{11} & \cdots & c_{1n}d_{1n} \\ \vdots & \ddots & \vdots \\ c_{m1}d_{m1} & \cdots & c_{mn}d_{mn} \end{bmatrix} \in \mathbb{R}^{m \times n}.$$

### A. Network model

By treating the vehicles in the platoon as nodes and the intervehicle communication as edges, a weighted directed graph  $\mathcal{G} = \mathcal{V}, \mathcal{E}, \mathcal{A}$  models the information flow topology (IFT) among the platoon. Within the digraph  $\mathcal{G}$ ,  $\mathcal{V} = \{1, 2, \dots, n\}$  denotes the nodes set and  $\mathcal{E} \subseteq \mathcal{V} \times \mathcal{V}$  represents edges set. Besides,  $\mathcal{A}$  is the weighted adjacent matrix with nonnegative elements defined as  $\mathcal{A} = [a_{ij}]_{n \times n}$  with  $a_{ii} = 0$  which denotes that the self-edge  $(i, i)$  is forbidden except as noted. Moreover, the edge  $(i, j)$  in  $\mathcal{E}$  means the communication exists between

vehicle  $i$  and vehicle  $j$  associated with weighted  $a_{ij}$ . Defining the degree matrix of  $\mathcal{G}$  as  $\mathcal{D} = \text{diag}\{d_1, d_2, \dots, d_n\}$ , with  $d_i = \sum_{j \in \mathcal{V}} a_{ij}$ .

### B. Integral inequality

Integral inequalities provide sufficient help for the study of lower bounds of quadratic function integrals in the stability analysis of state delayed systems [36, 37, 38]. Wirtinger Integral inequalities, being one of them, are considered to be effective and less conservative [39, 40]. Wirtinger Integral inequalities are a series of integral inequalities that adopt the integral of the function in estimating the integral of the derivative function. The Wirtinger Integral inequality is stated below:

**Lemma 1.** (Wirtinger Integral Inequality) [41]. Given a positive definite  $n \times n$  matrix  $R$ , the following inequality holds for any  $z \in C([-h, 0], \mathbb{R}^n)$  that satisfies  $z(-h) = z(0) = 0$ :

$$\int_{-h}^0 \dot{z}^T(u) R \dot{z}(u) du \geq \frac{\pi^2}{h^2} \int_{-h}^0 z^T(u) R z(u) du. \quad (1)$$

Although the Jensen inequality [42] is commonly employed in research to establish lower bounds of quadratic function integrals, its inherent conservatism can lead to less precise results. To obtain more accurate lower bounds, the Wirtinger Integral Inequality can be utilized, as highlighted in Remark 6.

In addition, we present another useful lemma that is motivated by the concept of reciprocally convex combination:

**Lemma 2.** [43]. Let  $n$  and  $m$  be positive integers,  $\alpha \in (0, 1)$  be a scalar,  $R > 0$  be a given  $n \times n$  matrix, and  $W_1$  and  $W_2$  be two  $n \times m$  matrices in  $\mathbb{R}^{n \times m}$ . The function  $\Theta(\alpha, R)$  is defined for all vectors  $\xi$  in  $\mathbb{R}^m$  as follows:

$$\Theta(\alpha, R) = \frac{1}{\alpha} \xi^T W_1^T R W_1 \xi + \frac{1}{1-\alpha} \xi^T W_2^T R W_2 \xi. \quad (2)$$

Then, if there exists a matrix  $X$  in  $\mathbb{R}^{n \times n}$  such that  $\begin{bmatrix} R & X \\ * & R \end{bmatrix} > 0$ , then the following inequality holds:

$$\min_{\alpha \in (0,1)} \Theta(\alpha, R) \geq \begin{bmatrix} W_1 \xi \\ W_2 \xi \end{bmatrix}^T \begin{bmatrix} R & X \\ * & R \end{bmatrix} \begin{bmatrix} W_1 \xi \\ W_2 \xi \end{bmatrix}. \quad (3)$$

### III. SYSTEM MODELING

In this scenario, a platoon of  $n$  CAVs are traveling along a single lane, and the intra-vehicle communication is carried out in accordance with the IFT protocol. Fig. 1 shows the schematic of the CAV platoon with typical four IFTs: Predecessor-Follower (PF), (b) Predecessor-Leader-Follower (PLF), (c) Bi-Directional (BD), and (d) Bi-Directional-Leader (BDL). Via intra-vehicle communication (e.g., C-V2X according to the meeting report from Federal Communications Commission [44]), all vehicles within the platoon exchange state information, such as absolute position, velocity, and acceleration, with their neighboring vehicles in accordance with the IFT protocol. An assumption made is that each CAV is fitted with the following components: i) an on-board radar for detecting potential collisions by measuring the gap distance between consecutive vehicles, ii) a GPS sensor for

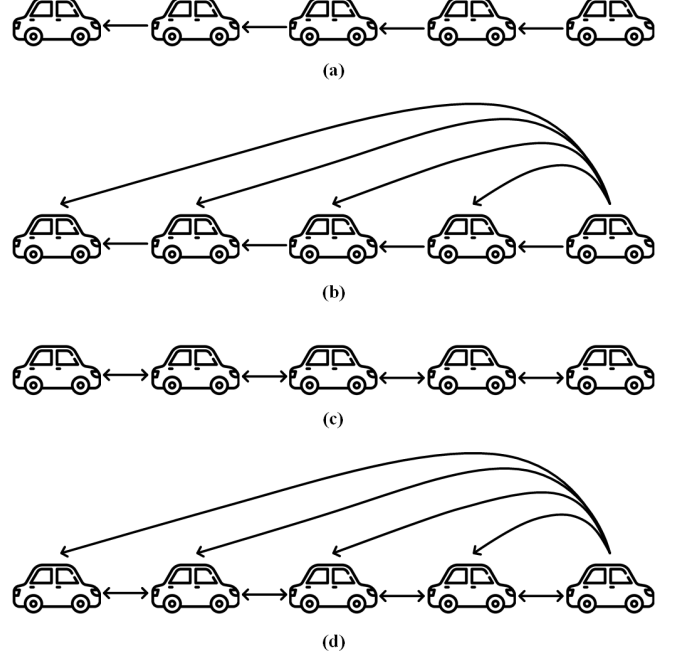


Fig. 1: The schematic of the CAV platoon with typical IFTs: (a) Predecessor-Follower (PF); (b) Predecessor-Leader-Follower (PLF); (c) Bi-Directional (BD); and (d) Bi-Directional-Leader (BDL).

obtaining the longitudinal position, iii) a wireless on-board unit that allows communication of relevant information with proximal vehicles via C-V2X communication [45], iv) an upper-level controller that calculates the desired longitudinal acceleration based on the obtained parameters, and v) a lower-level controller that determines the throttle and brake actuator inputs to follow the desired acceleration. This assumption is justifiable, as the sensing, communication, and actuation units listed above are standard features in modern CAVs and hence do not require any additional modifications to the existing vehicle configuration. It should be noted that the information obtained by the on-board radar regarding the surrounding environment only serves as a validation check in the event of communication unavailability or failure. This is because communication-based exchange of information is more efficient and provides more accurate data, rendering the use of radar as a supplementary measure rather than a primary source of information.

### A. Vehicle longitudinal dynamic Modeling

The longitudinal dynamics of a vehicle  $i$  can be mathematically formulated by accounting for various resistance forces that are influenced by the engine, throttle and brake actuators, drive train, transmission, and torque converter. The resulting model, based on the fundamental principles of Newton's second law, can be represented by the following equation:

$$m_i a_i(t) = f_i^e(t) - f_i^g(t) - f_i^w(t) - f_i^r(t), \quad (4)$$

where  $m_i$  stands for the unknown mass of vehicle  $i$ ;  $f_i^e(t)$  is the desired engine force acting on the vehicle  $i$ ;  $f_i^g(t)$ ,  $f_i^w(t)$ , and

$f_i^r(t)$  denote the gravity component parallel to the road surface, air resistance force, and rolling resistance force, respectively.

The nonlinearity of the system (4) makes it challenging to controller design. Therefore, a feedback control input in Appendix A is employed to convert it into a linear form [46]:

$$\tau_i \ddot{a}_i(t) + a_i(t) = u_i(t), \quad (5)$$

where  $u_i(t)$  denotes the control input of the lower-level controller, which can be interpreted as the desired acceleration of vehicle  $i$ ,  $\tau_i$  denotes the time constant that represents the delay caused by the engine actuator.

Reformulate Equation (5), the state space equation can be represented as:

$$\dot{x}_i(t) = Ax_i(t) + Bu_i(t), \quad (6)$$

$$\text{with } A = \begin{bmatrix} 0 & 1 & 0 \\ 0 & 0 & 1 \\ 0 & 0 & -\frac{1}{\tau_i} \end{bmatrix} \text{ and } B = \begin{bmatrix} 0 \\ 0 \\ \frac{1}{\tau_i} \end{bmatrix},$$

where  $x_i(t) = [p_i(t) \ v_i(t) \ a_i(t)]^T \in \mathbb{R}^3$  denotes the state vector of vehicle  $i$ .

Subject to limited communication, the inputs for vehicle  $i$  are controlled by an appropriate decentralized coupling protocol of communication information:

$$u_i = u_i(\underbrace{x_1(t-h(t)), \dots, x_i(t), \dots, x_n(t-h(t))}_n), \quad (7)$$

where  $h(t)$  represents the time-varying communication delay within the transmission range which is assumed to be influenced by the surrounding environment [47, 48, 49, 50, 51]. And it satisfies the following constraints:

$$h(t) \in [h_m, h_M], \quad \dot{h}(t) \in [d_m, d_M], \quad \forall t \geq 0, \quad (8)$$

where  $0 \leq h_m \leq h_M$  and  $d_m \leq d_M \leq 1$ .

Assuming that CAVs adopt the Constant Time Headway (CTH) policy, where CAVs maintain a desired time headway from the reference vehicle, we can formulate the cooperative tracking problem of vehicle  $i$  as follows:

$$\left\{ \begin{array}{l} \lim_{t \rightarrow \infty} \left\| \sum_{j=1}^n |p_i(t) - p_j(t-h(t)) + h_{ij}v_i(t)| \right\| = 0, \\ \lim_{t \rightarrow \infty} \left\| \sum_{j=1}^n |v_i(t) - v_j(t-h(t))| \right\| = 0, \quad \forall i = 1, \dots, N. \\ \lim_{t \rightarrow \infty} \left\| \sum_{j=1}^n |a_i(t) - a_j(t-h(t))| \right\| = 0. \end{array} \right. \quad (9)$$

where  $h_{ij} = -h_{ji}$  stands for the constant time headway between vehicle  $i$  and vehicle  $j$ .

By implementing a suitable distributed control strategy, the consensus objective stated in Equation (9) can be attained. Therefore, the vehicle  $i$  updates its dynamics via an onboard computation of the following decentralized coupling protocol:

$$u_i = - \sum_{j=1}^n a_{ij} k_{ij}^T \begin{bmatrix} p_i(t) - p_j(t-h(t)) + h_{ij}v_i(t) \\ v_i(t) - v_j(t-h(t)) \\ a_i(t) - a_j(t-h(t)) \end{bmatrix}, \quad (10)$$

where  $a_{ij}$  denotes the weight of edge  $(i, j)$  and  $a_{ij} = 0$  if there is no edge  $(i, j)$ ;  $k_{ij} = [\alpha_{ij} \ \beta_{ij} \ \gamma_{ij}]^T \in \mathbb{R}^{3 \times 1}$  presents the feedback control gain vector, with  $\alpha_{ij}$ ,  $\beta_{ij}$ , and  $\gamma_{ij}$  denoting the control gain of spacing, speed, and acceleration error, respectively.

### B. CAV platoon Modeling

To achieve consensus of systems (6) and (7) under the influence of the coupling protocol (10), it is necessary to reformulate the decentralized coupling protocol (10) as follows:

$$u_i = - \sum_{j=1}^n a_{ij} k_{ij}^T [\psi_{ij} x_i(t) - x_j(t-h(t))], \quad (11)$$

where  $\psi_{ij} = \begin{bmatrix} 1 & h_{ij} \\ & 1 \\ & & 1 \end{bmatrix}$  denotes the relationship between the states based on the CTH policy.

Therefore, the dynamics of the error system can be presented as:

$$\begin{cases} \dot{\tilde{p}}_i = \tilde{v}_i, \\ \dot{\tilde{v}}_i = \tilde{a}_i, \\ \dot{\tilde{a}}_i = -\frac{1}{\tau} \tilde{a}_i - \frac{1}{\tau} \sum_{j=1}^n a_{ij} k_{ij}^T (\psi_{ij} x_i(t) - x_j(t-h(t))). \end{cases} \quad (12)$$

From Equation (12), the dynamics of the closed-loop vehicular network can be reformulated using supermatrices, resulting in a more concise representation:

$$\dot{x}_i(t) = Ax_i(t) - B \sum_{j=1}^n a_{ij} k_{ij}^T (\psi_{ij} x_i(t) - x_j(t-h(t))). \quad (13)$$

**Theorem 3.** *The CAV platoon under CTH policy with time-varying communication delay can be modeled as a linear time-invariant state time-varying delay system:*

$$\begin{cases} \dot{X}(t) = \Psi X(t) + \Psi_d X(t-h(t)), & \forall t \geq 0 \\ X(t) = \phi(t), & \forall t \in [-h, 0] \end{cases} \quad (14)$$

with

$$\left\{
\begin{aligned}
\Psi &= A^* - B^* \mathcal{F} E_1 \in \mathbb{R}^{3n \times 3n} \\
\Psi_d &= B^* \mathcal{J} E_2 \in \mathbb{R}^{3n \times 3n} \\
A^* &= I_n \otimes A \in \mathbb{R}^{3n \times 3n} \\
B^* &= I_n \otimes B \in \mathbb{R}^{3n \times n} \\
\mathcal{K} &= [k_{ij}^T]_{n \times n} \\
\mathcal{H} &= \mathcal{A} \circ \mathcal{K} = [a_{ij} \otimes k_{ij}^T]_{N \times N} \in \mathbb{R}^{n \times 3n} \\
\mathcal{J} &= \text{diag} \{ \underbrace{\mathcal{D}_1, \mathcal{D}_2, \dots, \mathcal{D}_N}_{n} \} \in \mathbb{R}^{n \times 3n} \\
\mathcal{D}_i &= \underbrace{[a_{i1} k_{i1}^T, a_{i2} k_{i2}^T, \dots, a_{in} k_{in}^T]}_n \in \mathbb{R}^{1 \times 3n}, \forall i \in \mathcal{V} \\
\mathcal{F} &= \text{diag} \{ \underbrace{\mathcal{H}_1, \mathcal{H}_2, \dots, \mathcal{H}_N}_n \} \in \mathbb{R}^{n \times 3n^2} \\
\mathcal{H}_i &= \mathcal{D}_i \circ [\underbrace{\psi_{i1}, \psi_{i2}, \dots, \psi_{in}}_n] \in \mathbb{R}^{1 \times 3n}, \forall i \in \mathcal{V} \\
E_1 &= \text{diag} \{ \underbrace{I_1, I_1, \dots, I_1}_n \} \in \mathbb{R}^{3n^2 \times 3n} \\
E_2 &= \left[ \underbrace{I_2^T, \dots, I_2^T}_n \right]^T \in \mathbb{R}^{3n^2 \times 3n} \\
I_1 &= \left[ \underbrace{I_3^T, \dots, I_3^T}_n \right]^T \in \mathbb{R}^{3n \times 3} \\
I_2 &= I_{3n} \in \mathbb{R}^{3n \times 3n} \\
I_3 &= I_3 \in \mathbb{R}^{3 \times 3}
\end{aligned} \tag{15}
\right.$$

where  $X(t) = [x_1^T \ \dots \ x_n^T]^T \in \mathbb{R}^{3n}$  stands for the error state vector of the closed-loop vehicular network;  $\phi$  is the initial conditions;  $\Psi$  and  $\Psi_d$  are constant matrix according to their definitions.

#### IV. STABILITY ANALYSES

The Lyapunov-Krasovskii Stability Theorem is a commonly used method for analyzing stability in state delay systems. This approach is an extension of the second Lyapunov method, which is specifically designed for stability analysis [42]. It involves the use of "energy" functionals that are both positive definite and monotonically decreasing along the system trajectories. The statement of the Lyapunov-Krasovskii Theorem is presented below:

**Lemma 4.** (*Lyapunov-Krasovskii Stability Theorem*) [52]. Given system (14), suppose that  $f$  maps  $\mathbb{R} \times (\text{bounded sets in } \mathbb{R}^n \times C)$  into bounded sets in  $\mathbb{R}^n$ , and that  $u, v, w : \mathbb{R}_+ \rightarrow \mathbb{R}_+$  are continuous nondecreasing functions, where additionally  $u(s)$  and  $v(s)$  are positive for  $s > 0$ , and  $u(0) = v(0) = 0$ . If there exists a functional  $V : \mathbb{R} \times \mathbb{R}^n \times C \rightarrow \mathbb{R}$  such that

$$\begin{cases} u(|\phi(0)|) \leq V(t, \phi) \leq v(|\phi|_h), \\ \dot{V}(t, \phi) \leq -w(|\phi(0)|). \end{cases} \tag{16}$$

Then the trivial solution of the system (14) is uniformly stable. If  $w(s) > 0$  for  $s > 0$ , then it is uniformly asymptotically stable. If, in addition,  $\lim_{s \rightarrow \infty} u(s) = +\infty$ , then it is globally uniformly asymptotically stable. Such a functional  $V$  is called a Lyapunov-Krasovskii functional (LKF).

Lemma 4 aims to establish a positive definite functional whose time derivative is negative definite along the trajectories of the system (14). This forms the core idea behind the lemma. In the context of the stability analysis of such systems using LKF, several types of functionals have been provided in the literature. Among them, an integral quadratic term is one of the most relevant components of LKF [53]:

$$V(X_t) = \int_{0-h}^0 \int_\theta^0 \dot{X}_t^T(s) R \dot{X}_t(s) ds d\theta, \tag{17}$$

where  $\dot{X}_t(s) = \dot{X}(t+s)$  denotes the state of the state delay system,  $R > 0$  and  $h > 0$ .

The positivity of LKF (17) is ensured by  $R > 0$ . Then another that needs to be clarified is the negation of its derivative. Differentiating this term with respect to the time  $t$ , we get:

$$\dot{V}(X_t) = h \dot{X}^T(t) R \dot{X}(t) - \int_{-h}^0 \dot{X}^T(s) R \dot{X}(s) ds. \tag{18}$$

To transform Equation (18) into a suitable LMI framework, an over-approximation process of the integral terms is required as they cannot be readily converted using the quadratic formulation discussed previously. Consequently, the current task is to derive a new lower bound of integral quadratic terms in the following format:

$$F(\omega) = \int_{-h}^0 \omega^T(s) R \omega(s) ds, \tag{19}$$

where  $\omega$  is a continuous function from  $[a, b] \rightarrow \mathbb{R}^n$  and consequently integrable.

**Corollary 5.** Given a positive definite matrix  $R$ , the following inequality holds for all continuous functions  $\omega : [a, b] \rightarrow \mathbb{R}^n$ :

$$F(\omega) \geq \frac{1}{h} \left( \int_{-h}^0 \omega(u) du \right)^T R \left( \int_{-h}^0 \omega(u) du \right) + \frac{3}{h} \Omega^T R \Omega, \tag{20}$$

$$\text{where } \Omega = \int_{-h}^0 \omega(s) ds - \frac{2}{h} \int_{-h}^0 \int_{-h}^s \omega(r) dr ds.$$

*Proof:* We first construct the function  $z$  for all  $u \in [a, b]$  as:

$$z(u) = \int_{-h}^u \omega(s) ds - \frac{u+h}{h} \int_{-h}^0 \omega(s) ds - \frac{(-u)(u+h)}{h^2} \Theta, \tag{21}$$

where  $\Theta$  is a constant vector of  $\mathbb{R}^n$  to be defined. Moreover, the function  $z(u)$  (21) satisfies the constraints of Lemma 1, that is  $z(0) = z(-h) = 0$  according to its definition.

Then, calculating the left-hand-side of the inequality mentioned in Lemma 1 yields:

$$\begin{aligned}
\int_{-h}^0 \dot{z}^T(u) R \dot{z}(u) du &= 2 \int_{-h}^0 \left( \frac{(-h-2u)}{h^2} \right) du \Theta^T R \left( \int_{-h}^0 \omega(u) du \right) \\
&+ \int_{-h}^0 \left( \frac{(h+2u)}{h^2} \right)^2 du \Theta^T R \Theta - 2 \Theta^T R \int_{-h}^0 \left( \frac{-h-2u}{h^2} \right) \omega(u) du \\
&+ \int_{-h}^0 \omega^T(u) R \omega(u) du - \frac{1}{h} \left( \int_{-h}^0 \omega(u) du \right)^T R \left( \int_{-h}^0 \omega(u) du \right).
\end{aligned} \tag{22}$$

Substituting  $\int_{-h}^0 -h-2u du = 0$  and applying integration by

parts, Equation (22) can be simplified as follows:

$$\begin{aligned} \int_{-h}^0 \dot{z}^T(u) R \dot{z}(u) du &= \int_{-h}^0 \omega^T(u) R \omega(u) du \\ -\frac{1}{h} \left( \int_{-h}^0 \omega(u) du \right)^T R \left( \int_{-h}^0 \omega(u) du \right) \\ -\frac{3}{(b-a)} \Omega^T R \Omega + \frac{1}{3(b-a)} (\Theta + 3\Omega)^T R (\Theta + 3\Omega). \end{aligned} \quad (23)$$

Substituting  $\int_{-h}^0 z(u) du = -\frac{h}{6}(\Theta + 3\Omega)$  and applying Lemma 1, it yields:

$$\begin{aligned} F(\omega) &\geq \frac{1}{h} \left( \int_{-h}^0 \omega(u) du \right)^T R \left( \int_{-h}^0 \omega(u) du \right) + h \Omega^T R \Omega \\ &\quad + \frac{\pi^2 - 12}{36h} (\Theta + 3\Omega)^T R (\Theta + 3\Omega). \end{aligned} \quad (24)$$

Given that  $\frac{\pi^2 - 12}{36h} > 0$ , the third term on the right-hand side of the inequality (24) is positive definite, regardless of the selection of  $\Theta$ . Moreover, the inequality is equivalent to equality if and only if  $\Theta = -3\Omega$ . Furthermore, the definite positiveness of  $F(\omega)$  is guaranteed by  $R > 0$ . This concludes the proof. ■

**Remark 6.** Note that the first term to the right of Inequality (20) is Jensen inequality [42]. Since the second term is definite positive, the lower bound of the integral is clearly higher than the result obtained through Jensen inequality. Therefore, with Wirtinger-Based on Integral Inequality, more accurate stability conditions can be obtained.

According to Inequality (18), another lower bound needed to be determined is the case of  $F(\hat{\omega})$ . Therefore, Corollary 5 is rewritten as follows:

**Corollary 7.** Given a positive definite matrix  $R$ , all continuously differentiable functions  $\omega : [a, b] \rightarrow \mathbb{R}^n$  satisfy the subsequent inequality:

$$F(\omega) \geq \frac{1}{h} (\omega(0) - \omega(-h))^T R (\omega(0) - \omega(-h)) + \frac{3}{h} \tilde{\Omega}^T R \tilde{\Omega}, \quad (25)$$

where  $\tilde{\Omega} = \omega(0) + \omega(-h) - \frac{2}{h} \int_a^b \omega(u) du$ .

The subsequent stability theorem is presented below:

**Theorem 8.** Assuming the existence of  $P \in \mathbb{S}_{3n}^+$ , three matrices  $S, R, Q \in \mathbb{S}^{n+}$ , and  $X \in \mathbb{S}^{2n}$ , the ensuing LMIs hold for  $h = h_m, h_M$  and  $\dot{h} = d_m, d_M$ .

$$\Phi_1(h, \dot{h}) = \Phi_0(h, \dot{h}) - \frac{1}{h_M} \Gamma^T \Phi_2 \Gamma < 0, \quad (26)$$

$$\Phi_2 = \begin{bmatrix} \tilde{R} & X \\ * & \tilde{R} \end{bmatrix} > 0, \quad (27)$$

where

$$\Phi_0(h, \dot{h}) = \text{He} \left( G_1^T(h) P G_0(\dot{h}) \right) + \hat{S} + \hat{Q}(\dot{h}) + h_M G_0^T(\dot{h}) \hat{R} G_0(\dot{h});$$

$$\Gamma = \begin{bmatrix} K_1^T & K_2^T \end{bmatrix}^T;$$

$$K_1 = \begin{bmatrix} I & -I & 0 & 0 & 0 \\ I & I & 0 & -2I & 0 \end{bmatrix};$$

$$K_2 = \begin{bmatrix} 0 & I & -I & 0 & 0 \\ 0 & I & I & 0 & -2I \end{bmatrix};$$

$$\hat{Q}(\dot{h}) = \text{diag} \left( Q, -(1 - \dot{h})Q, 0_{3n} \right);$$

$$\hat{S} = \text{diag} (S, 0, -S, 0_{2n});$$

$$\hat{R} = \text{diag} (R, 0_{3n});$$

$$\tilde{R} = \text{diag} (R, 3R);$$

$$G_0(\dot{h}) = \begin{bmatrix} \Psi & \Psi_d & 0 & 0 & 0 \\ I & -(1 - \dot{h})I & 0 & 0 & 0 \\ 0 & (1 - \dot{h})I & -I & 0 & 0 \\ I & 0 & 0 & 0 & 0 \\ 0 & 0 & 0 & hI & 0 \\ 0 & 0 & 0 & 0 & (h_M - h)I \end{bmatrix};$$

Then the system (14) is asymptotically stable for all delay function  $h$  satisfying (8).

*Proof:* We first construct the LKF as:

$$\begin{aligned} V(h, x_t, \dot{x}_t) &= \tilde{x}^T(t) P \tilde{x}(t) + \int_{-h(t)}^0 x^T(s) Q x(s) ds \\ &\quad + \int_{-h_M}^0 x^T(s) S x(s) ds + \int_{-h_M}^0 \int_{\theta}^0 \dot{x}^T(s) R \dot{x}(s) ds d\theta, \end{aligned} \quad (28)$$

$$\text{where } \tilde{x}(t) = \left[ x^T(t), \int_{-h(t)}^0 x^T(s) ds, \int_{-h_M}^{-h(t)} x^T(s) ds \right]^T.$$

The positivity of LKF (28) is guaranteed by  $P > 0$ ,  $Q > 0$ ,  $S > 0$ , and  $R > 0$ . Consequently, the negation of its derivative needs to be elucidated. Upon differentiating the functional (18) along the trajectories of (14), we obtain:

$$\dot{V}(h, x_t, \dot{x}_t) = \zeta_1^T(t) \Phi_0(h, \dot{h}) \zeta_1(t) - \int_{-h_M}^0 \dot{x}^T(s) R \dot{x}(s) ds, \quad (29)$$

$$\text{where } \zeta_1(t) = \begin{bmatrix} x(t) \\ x(t - h(t)) \\ x(t - h_M) \\ \frac{1}{h(t)} \int_{-h(t)}^0 x(s) ds \\ \frac{1}{h_M - h(t)} \int_{-h_M}^{-h(t)} x(s) ds \end{bmatrix}.$$

Notice the Equation (29) can be obtained by substituting  $\tilde{x}(t) = G_1(h) \zeta_1(t)$  and  $\dot{\tilde{x}}(t) = G_0(\dot{h}) \zeta_1(t)$  into the partial differential of Equation (28).

Then split the integral interval of Equation (29) into two parts:  $[-h_M, -h(t)]$  and  $[-h_M, 0]$ , and apply Corollary 7 respectively to get:

$$\begin{aligned} - \int_{t-h_M}^t \dot{x}^T(s) R \dot{x}(s) ds &\leq \\ - \zeta_1^T(t) \left( \frac{1}{h(t)} K_1^T \tilde{R} K_1 + \frac{1}{h_M - h(t)} K_2^T \tilde{R} K_2 \right) \zeta_1(t). \end{aligned} \quad (30)$$

Given the constraint of Lemma 2, assuming the existence of  $X$  such that  $\Phi_2 > 0$ , we can conclude that the ensuing inequality holds true:

$$- \int_{t-h_M}^t \dot{x}^T(s) R \dot{x}(s) ds \leq -\frac{1}{h_M} \zeta_1^T(t) \Gamma^T \Phi_2 \Gamma \zeta_1(t), \quad (31)$$

Substituting Inequality (31) into Equation (29), it yields:

$$\begin{aligned} \dot{V}(h, x_t, \dot{x}_t) &\leq \zeta_1^T(t) \Phi_0(h, \dot{h}) \zeta_1(t) - \frac{1}{h_M} \zeta_1^T(t) \Gamma^T \Phi_2 \Gamma \zeta_1(t) \\ &= \zeta_1^T(t) \left( \Phi_0(h, \dot{h}) - \frac{1}{h_M} \Gamma^T \Phi_2 \Gamma \right) \zeta_1(t) \\ &= \zeta_1^T(t) \Phi_1(h, \dot{h}) \zeta_1(t). \end{aligned} \quad (32)$$

The inequality stated in Equation (32) guarantees the negative definiteness of  $\dot{V}(h, x_t, \dot{x}_t)$  by constraining  $\Phi_1(h, \dot{h}) < 0$ . It is worth noting that the matrix  $\Phi_1(h, \dot{h})$  is affine, and therefore convex with respect to  $h(t)$  and  $\dot{h}(t)$ . Thus, to ensure  $\Phi_1(h, \dot{h}) < 0$  holds, it is necessary and sufficient to restrict it to the vertices of the intervals  $[0, h_M] \times [d_m, d_M]$ .

In summary, the negativity of  $\dot{V}(h, x_t, \dot{x}_t)$  is guaranteed if there exists a matrix  $X$  such that  $\Phi_2 > 0$  and  $\Phi_1(h, \dot{h}) < 0$  holds for all  $(h, \dot{h}) \in [0, h_M] \times [d_m, d_M]$ . This concludes the proof. ■

**Remark 9.** The central concept of the Lyapunov-Krasovskii stability theorem is that it is not imperative to establish the negative definiteness of  $V(t, x(t))$  along all system trajectories. Instead, it is adequate to ensure its negative definiteness for solutions that tend to escape the vicinity of  $V(t, x(t)) \leq c$  of the equilibrium. Appendix B provides a comprehensive theoretical analysis of this concept.

**Remark 10.** The code for constructing the LMIs in Theorem 8 has been uploaded to GitHub for subsequent research. The corresponding URL is attached in Appendix C for further reference.

## V. NUMERICAL ANALYSES

In this section, extensive numerical simulations and analyses on the tracking performance and safety conditions of CAV platoon with different feedback control gains employing the PLF are conducted to illustrate the main results. In addition, the tracking performances of the CAV platoon employing the other three IFTs are also investigated.

### A. Numerical Setup

For a comprehensive performance evaluation analysis, a CAV platoon consisting of 5 interconnected CAVs using the PLF as shown in Fig.1 (b) is considered. The Leader CAV drives under a given speed profile while the other CAVs drive under the control strategy. It is worth clarifying that each CAV in the platoon communicates only with the neighbors in the PLF. Additionally, the control parameters need to be set according to the specific control strategy in practice. For further analysis, parameters for both network and traffic simulation are set in Table I, for simplicity but without loss of generality. It should be noted that the weights of the weighted adjacency matrix are set to  $a_{ij} = \frac{1}{d_i}, \forall (i, j) \in \mathcal{E}$  in order to denote that the information of each neighbor has an equal impact on the control decision. As for the time-varying delay, the time-varying equation is given below in the form of the Bessel function of the first kind, whose time-varying curve is shown in Fig. 2, satisfying the constraint in Equation (8):

$$J_{40}(t) = \sum_{k=0}^{\infty} \frac{(-1)^k}{k!(k+40)!} \left( \frac{t+30}{2} \right)^{2k+40}, \quad t \geq 0. \quad (33)$$

Moreover, for the sake of evaluating the tracking performance under the PLF with different feedback control gains of the CAV platoon, we adopt two representative leader maneuvers, namely:

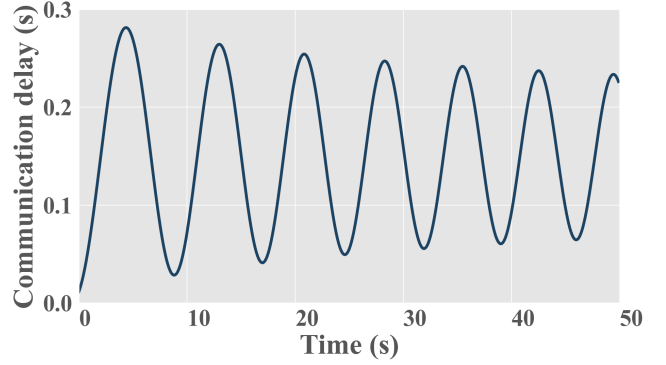


Fig. 2: The curve of time-varying communication delay.

TABLE I: Network and traffic simulation parameters.

Parameters	Value
Platoon size $n$	5 vehicles
Vehicle length $L$	5 [m]
Engine actuator delay $\tau_i$	0.2 [s] <sup>1</sup>
Weight of edge $(i, j)$ $a_{ij}$	$\frac{1}{d_i}$
Minimum communication delay $h_m$	0 [m]
Maximum communication delay $h_M$	0.3 [m]
Minimum communication delay slope $d_m$	-0.1
Maximum communication delay slope $d_M$	0.1

<sup>1</sup> [54, 55]

- 1) **Trapezoidal signal:** The leader suddenly decelerates to  $14.6\text{m/s}$  at  $-0.15\text{m/s}^2$  and keeps it for  $36\text{s}$ . Then the leader accelerates back to  $20\text{m/s}$  at  $0.3\text{m/s}^2$  (see Fig. 3(a, b)).
- 2) **Oscillation signal:** The leader suddenly accelerates to  $23.6\text{m/s}$  in  $12\text{s}$  and keeps the velocity for  $15\text{s}$ . Then the leader decelerates to  $16.4\text{m/s}$  in  $12\text{s}$  and accelerates back to  $20\text{m/s}$  in  $12\text{s}$  (see Fig. 3(c, d)).

### B. Numerical analyses of the CAV platoon under the PLF

In this subsection, the analysis focuses on the CAV platoon that employs the PLF, with the same control parameters for each CAV in the platoon, meeting the requirements of Theorem 8. The impact of tracking performance with different feedback control gains is investigated by selecting four feedback control gains:

- 1) *Parameter I:*  $k_i = [0.3, 0.3, 0.3]^T$ ;
- 2) *Parameter II:*  $k_i = [1, 0.3, 0.3]^T$ ;
- 3) *Parameter III:*  $k_i = [0.3, 1, 0.3]^T$ ;
- 4) *Parameter IV:*  $k_i = [0.3, 0.3, 1]^T$ .

Moreover, the desired time headway is set to  $h_i = 0.6\text{s}$ . Corresponding matrixes  $P, S, Q, R$ , and  $X$  are provided in Appendix C. Moreover, a thorough analysis is carried out on the tracking performance and safety conditions.

1) *Tracking performance analyses:* After the formation of the CAV platoon and achieving the equilibrium state where the tracking error is zero, the tracking performance of the four feedback control gains under investigation is evaluated using

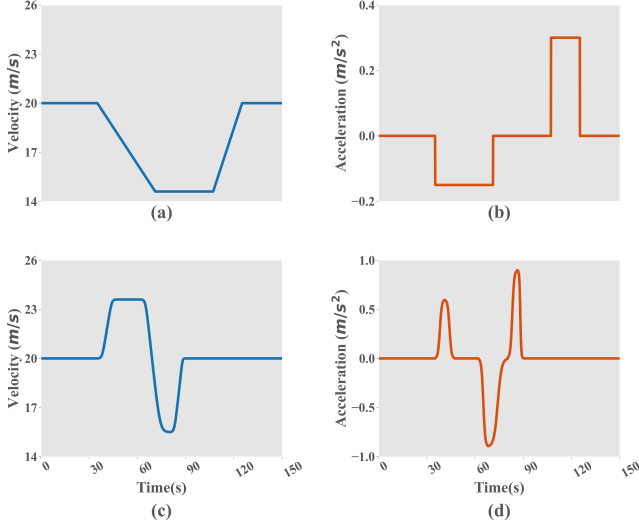


Fig. 3: The two representative leader maneuvers: (a) and (b) denotes the velocity and acceleration of the trapezoidal signal, respectively; (c) and (d) denote the velocity and acceleration of the oscillation signal, respectively.

the trapezoidal signal displayed in Fig.3(a,b) as the leader maneuver. The results are presented in Fig.4, which shows the tracking of the leader motion by the different CAVs in the platoon.

As expected from the theoretical results, all CAVs can smoothly track the leader motion with a steady-state error of 0. Transient variations in the leader motion can cause abrupt changes in the tracking error, which diminish over time thanks to stability. Additionally, the effect of different feedback control gains on the tracking performance differs, as demonstrated by comparing the results of the four control gains. Increasing the gain of the spacing and velocity errors significantly reduces the overshoot of the acceleration curve, especially in the case of the velocity error gain, where the overshoot is effectively suppressed. However, increasing the gain of the spacing error leads to fluctuations in the acceleration curve, possibly due to time-varying delay. On the other hand, increasing the gain of the acceleration error negatively affects the tracking performance due to drastic fluctuations, even though stability is maintained. Therefore, in terms of control parameter selection, increasing the gain of the velocity error within a suitable range can improve the tracking performance to a certain extent.

Furthermore, the tracking performance of the four feedback control gains has also been evaluated under the oscillation signal defined in Fig. 3(c, d). Fig.5 illustrates the corresponding tracking performance of the four feedback control gains. Under the oscillation signal, all cases under the four feedback control gains still maintain excellent tracking performance, where each vehicle adjusts to changes in leader motion and returns to the equilibrium state with zero steady-state error. Additionally, a similar phenomenon and conclusion as in Fig. 4 can be observed, namely that increasing the gain of spacing and velocity errors can benefit tracking performance while increasing the gain of acceleration errors does not necessarily

Furthermore, to complement the analysis on stability via tracking performance, we have investigated two widely accepted indicators, namely Setting Time (ST) and Number of Oscillations (NOO), for evaluating the transient response performance of different feedback control gains. ST refers to "the time required for the response curve to reach and stay within a range of a certain percentage (2%) of the final value", while NOO refers to "the number of deviations of the response curve from the final value caused by errors in the setting time". Both ST and NOO are important measures of transient response, with ST representing the speed in achieving equilibrium and NOO representing the accuracy and comfort of the response. Since the investigation focuses on the differences in the transient response of different feedback control gains, the form of the leader motion has little impact, and thus the results are analyzed here only for the Trapezoidal signal case.

Fig. 6 compares the effects of different feedback control gains on two transient response indicators: Setting time (ST) and Number of oscillations (NOO). The results indicate that different control gains have a significant impact on transient response. Specifically, Parameter II and Parameter III show smaller ST and NOO than Parameter I, indicating that increasing the gain of spacing and velocity errors is effective in reducing velocity fluctuations and time from perturbation to equilibrium, thereby improving driving comfort and safety. However, increasing the gain of acceleration error, as in Parameter IV, does not improve transient response. Moreover, for all control gain cases, the ST increases and NOO decreases with increasing vehicle index, suggesting that larger CAV platoons have less velocity fluctuation from perturbation to equilibrium, albeit with longer recovery times. Notably, Parameter III results in NOO=0, indicating no overshoot during transient response, and thus, performs well in terms of safety and comfort.

2) *Safety analyses considering hard braking maneuver:* To further assess safety across various driving scenarios and feedback control gains, we conduct a quantitative analysis to examine the potential emergence of critical driving situations for all feedback control gains under investigation. This analysis utilizes the well-established safety indicator, Deceleration Rate to Avoid the Crash (DRAC), which has been extensively studied in the literature [56, 57]. This indicator presents the deceleration rate needed to be applied by a vehicle to avoid a collision with another vehicle which can be defined for each vehicle  $i$  at the time  $t$  as follows:

$$DRAC_i(t) = \frac{(v_i(t) - v_{i-1}(t))^2}{2(p_{i-1}(t) - p_i(t) - L)}. \quad (34)$$

Furthermore, an additional scenario was considered to evaluate safety across various driving scenarios and feedback control gains, specifically a hard braking maneuver where the Leader decelerates from 20 m/s to 0 m/s within 20 s. The reaction of the CAV platoon to this scenario for the four feedback control gains under investigation is displayed in Fig.7. Notably, the CAVs in the platoon accurately track the Leader motion and decelerate to 0 m/s without collision under each control gain. The DRAC of different CAVs under different control

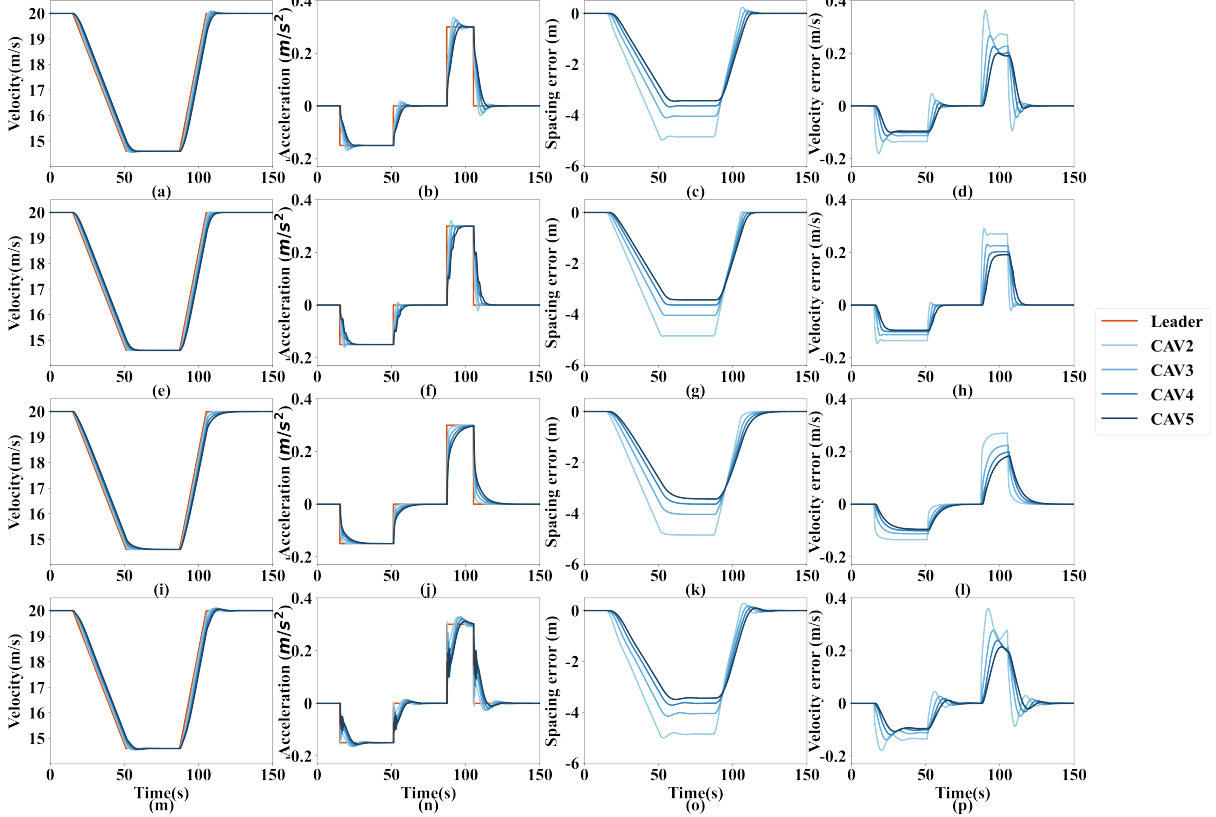


Fig. 4: Tracking performance of the CAV platoon for the Trapezoidal signal in Fig. 3(a,b) under the four feedback control gains: (a), (b), (c), and (d) present tracking results under Parameter I, including the velocity, tracking error of spacing, tracking error of velocity, and tracking error of acceleration, respectively; (e), (f), (g), and (h) show the case under Parameter II; (i), (j), (k), and (l) denote the case under Parameter III; (m), (n), (o), and (p) show the case under Parameter IV.

gains in the hard braking maneuver is presented as boxplots in Fig. 8, with the Leader's DRAC omitted due to its lack of a predecessor. The second through fifth CAVs in the platoon are denoted as CAV2, CAV3, CAV4, and CAV5, respectively.

From Fig. 8, a notable phenomenon can be observed by comparing the boxplots. The median DRAC of all CAVs under Parameter II and Parameter III is significantly lower than that under Parameter I and Parameter IV, which is consistent with the rough results obtained in the tracking performance analyses. This finding suggests that increasing the gain of spacing and velocity errors can maintain better safety compared to increasing the gain of acceleration error. Furthermore, a second conclusion can be drawn by comparing different CAVs under the same feedback control gain. Despite the control parameters being identical, the position of a CAV in the platoon influences the safety conditions.

### C. Numerical analyses of the alternative IFTs

In this subsection, the parameters in Table I are still adopted for both network and traffic simulation. Moreover, the control parameters are set to  $k_i = [0.3, 0.3, 0.3]^T$  and  $h_i = 0.6s$ . The difference is that the section mainly analyzes the tracking performance of the CAV platoon employed by PF, BD or BDL. It is worth mentioning that the control parameters chosen here

still exist matrixes  $P, S, Q, R$ , and  $X$  satisfy the Theorem 8, which can be found in Appendix C.

As in Section V-B1, the Trapezoidal signal defined in Section V-A is employed to investigate the tracking performance of different IFTs. The tracking performance of the CAV platoon is presented in Fig. 9.

Alternative IFTs have also been evaluated, and they have demonstrated favorable tracking performance. A similar phenomenon can be observed that the transient response from tracking Leader motion decreases gradually, thanks to stability. It is worth noting that for the case of BD and BDL, the tracking process is smooth; on the contrary, there are significant fluctuations in the tracking process for the case of PF, as disclosed in the recent technical literature [58].

Similarly, ST and NOO are analyzed to investigate the specific effects of different IFTs on the transient response, and the results are demonstrated in Fig. 10. It can be found that the case under BD has a significantly higher ST than the cases under the other three IFTs. Moreover, although the ST of the cases under all IFTs increases with the increase of the vehicle index, only the case under PF increases significantly while the cases under the other IFTs increase very slightly. One conclusion can be drawn that the CAV platoon with PLF and BDL recovers from the perturbation to the equilibrium state more quickly than PF and BD. In fact, this phenomenon

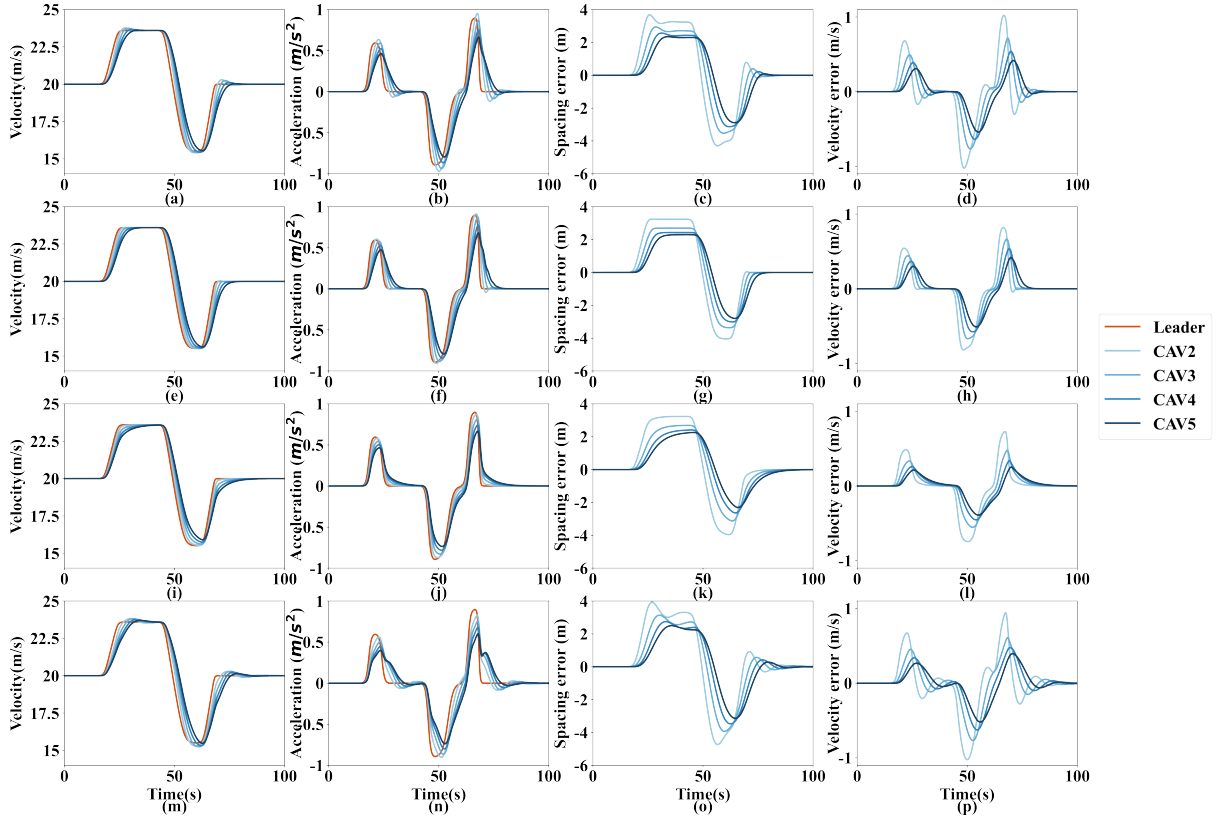


Fig. 5: Tracking performance of the CAV platoon for the Oscillation signal in Fig. 3(c,d) under the four feedback control gains: (a), (b), (c), and (d) present tracking results under Parameter I, including the velocity, tracking error of spacing, tracking error of velocity, and tracking error of acceleration, respectively; (e), (f), (g), and (h) show the case under Parameter II; (i), (j), (k), and (l) denote the case under Parameter III; (m), (n), (o), and (p) show the case under Parameter IV.

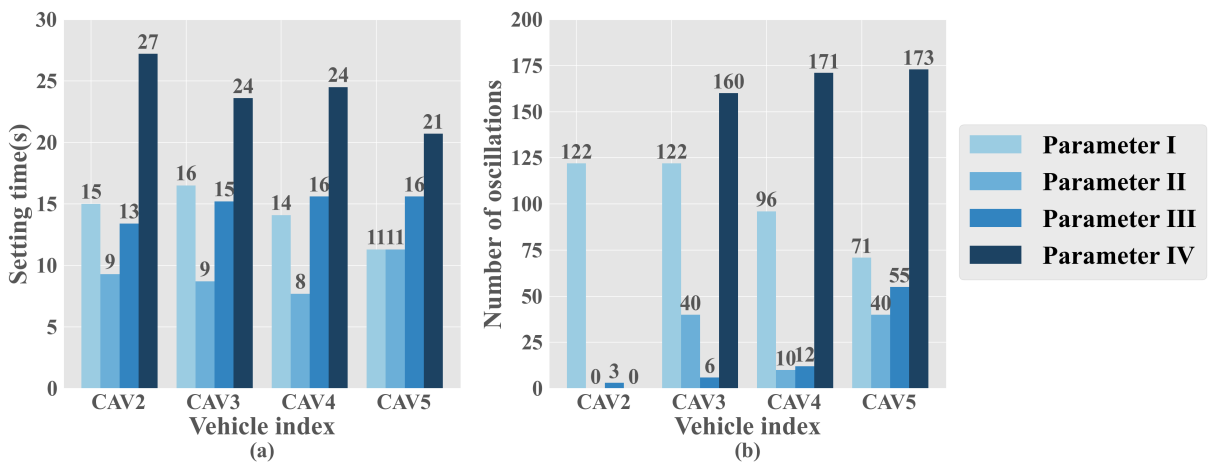


Fig. 6: Indicators for evaluating the transient response of each CAV among the CAV platoon under the four feedback control gains: (a) the case of setting time; (b) the case of the number of oscillations.

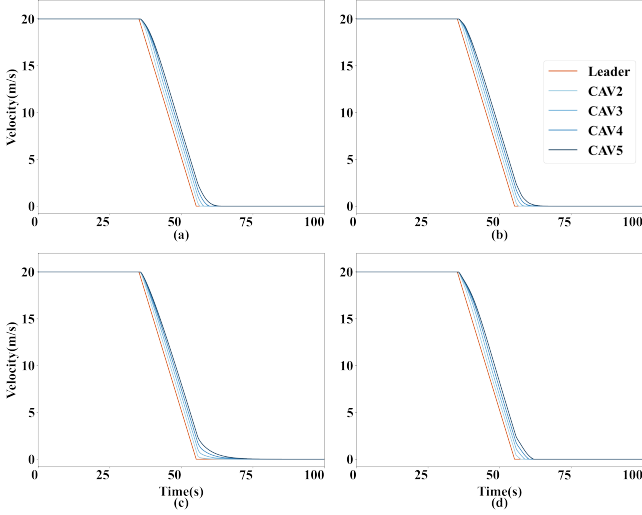


Fig. 7: Tracking performance for a hard braking maneuver for each feedback control gain under investigation: (a) Parameter I; (b) Parameter II; (c) Parameter III; (d) Parameter IV.

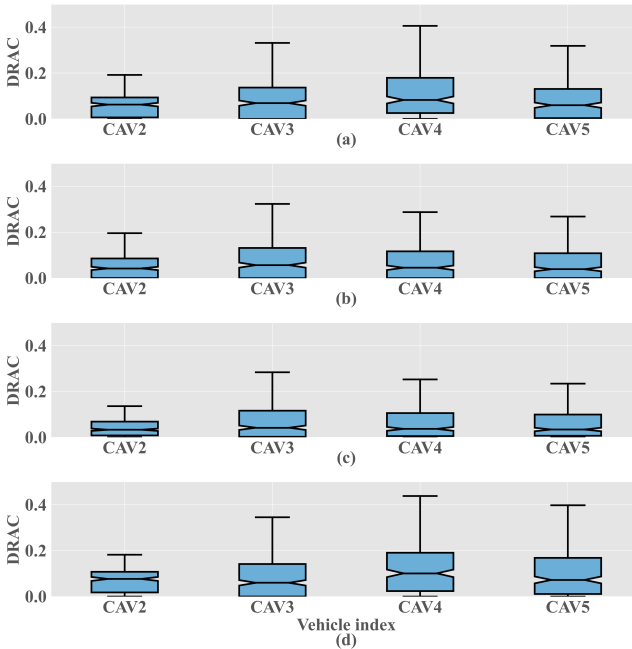


Fig. 8: The DRAC boxplots for each CAV of each feedback control gain under investigation: (a) Parameter I; (b) Parameter II; (c) Parameter III; (d) Parameter IV.

arises due to the direct communication with the leader, which effectively mitigates hard oscillations during transients.

On the other hand, as the vehicle index increases, for the cases under PLF, BD, and BDL, the NOO decreases, while for the cases under PF, the NOO increases. Furthermore, of the other three IFTs, the case under BD has the largest NOO, and the case under BDL has the smallest. In general, the transient performance can be significantly enhanced by communicating with the leader and bi-directional communication.

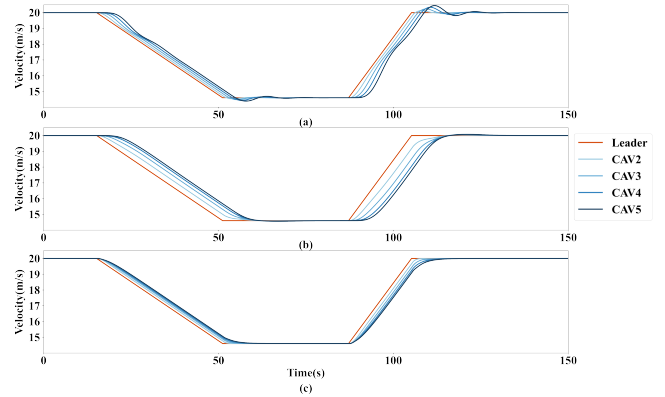


Fig. 9: Tracking performance of the CAV platoon for the Trapezoidal signal in Fig. 3(a,b) under the alternative three IFTs: (a) presents tracking results under PF; (b) presents tracking results under BD; (c) denotes the case under BDL.

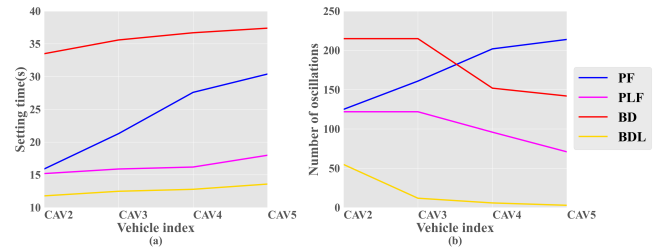


Fig. 10: Indicators for evaluating the transient response of each CAV among the CAV platoon under the four IFTs: (a) the case of setting time; (b) the case of the number of oscillations.

## VI. CONCLUSION AND FUTURE WORK

In this paper, a generic supermatrix modeling approach is proposed for the CAV platoon, which considers time-varying communication delay. The communication relationships within a CAV platoon, generally defined by IFT, are described using graph theory, and the linear time-invariant state time-varying delay system corresponding to the CAV platoon that employs a CTH control strategy is modeled using supermatrices. Based on the properties of the linear time-invariant state time-varying delay system, a novel stability condition of the generic CAV platoon is derived by applying the Wirtinger-Based Integral Inequality and Lyapunov-Krasovskii Stability Theorem. Furthermore, extensive numerical analyses are conducted to comprehensively evaluate the tracking performance and safety conditions of four control parameters, providing guidance for the selection of control parameters. Lastly, a comparison of the tracking performance between the CAV platoon employing different IFTs is presented, shedding light on the selection of IFTs.

The following conclusions can be drawn through numerical analysis:

- 1) A stability condition that considers time-varying delay for the CAV platoon can be obtained using the Lyapunov-Krasovskii stability theorem and Wirtinger-Based Integral Inequality.
- 2) The CAV platoon, employing the investigated control pa-

rameters and IFTs, can track the leader motion smoothly, maintain safe conditions in various scenarios, and guarantee stability.

- 3) Increasing the gain of spacing and velocity errors benefits both tracking performance and safety conditions, while increasing the gain of acceleration errors does not.
- 4) Communicating with the leader and bi-directional communication can significantly enhance tracking and transient performance from the IFT perspective.

However, we acknowledge that the vehicle behavior in the simulation is only a simplification of reality, and further field experiments are needed for providing a more accurate analysis of the tracking performance. Likewise, the time-varying delay function applied in this paper is an assumed Bessel function satisfying the condition that both the delay and its derivative are bounded, which does not fit the actual time-varying delay perfectly. Therefore, corresponding field experiments should also be conducted to provide insights into the time-varying relationship of communication delays. Furthermore, the control parameter scheme that yields the optimal tracking performance should be further investigated through theoretical research and field experiments. Future research should also be directed toward designing novel control strategies to enable smoother and safer tracking performance.

## APPENDIX

### APPENDIX A. FEEDBACK CONTROL FOR LINEARIZATION

In this appendix, we provide the linearization of the longitudinal vehicle dynamic in Equation (4). The functions of the lumped uncertain resistance forces, including  $f_i^g(t)$ ,  $f_i^w(t)$ , and  $f_i^r(t)$  are expressed as follows:

$$\begin{cases} f_i^g(t) = m_i g \sin(\theta_i(t)), \\ f_i^w(t) = \frac{1}{2} \rho C_D A_F (v_i(t) + v_w(t))^2, \\ f_i^r(t) = \mu_R m_i g \cos(\theta_i(t)). \end{cases} \quad (35)$$

where  $g = 9.81 \text{m/s}^2$  denotes the acceleration of gravity;  $\theta_i(t)$  is the inclination angle of the road;  $\rho$  denotes the air density;  $C_D$  is the aerodynamic drag coefficient;  $A_F$  represents the maximal cross-sectional/frontal area of the vehicle;  $v_w(t)$  denotes the uncertain headwind speed;  $\mu_R$  is the coefficient of rolling resistance.

The desired engine dynamic is modeled as follows:

$$(\tau_i s + 1) F_i^e = U_i. \quad (36)$$

Adopting the inverse Laplace transformation on Equation (36) arrives at:

$$\dot{f}_i^e(t) = \frac{u_i(t)}{\tau_i} - \frac{f_i^e(t)}{\tau_i}. \quad (37)$$

Substituting Equation (4) into Equation (37) and differentiating both sides of Equation (37) with respect to time, we

get:

$$\begin{aligned} \ddot{a}_i(t) &= \frac{\dot{f}_i^e(t)}{m_i} - \frac{\dot{f}_i^g(t)}{m_i} - \frac{\dot{f}_i^{i\omega}(t)}{m_i} - \frac{\dot{f}_i^r(t)}{m_i} \\ &= \frac{u_i(t)}{m_i \tau_i} \\ &\quad - \frac{a_i(t) + g \sin(\theta_i(t)) [1 - \tau_i \mu_R \dot{\theta}_i(t)] + g \cos(\theta_i(t)) [1 + \tau_i \dot{\theta}_i(t)]}{\tau_i} \\ &\quad - \frac{\frac{1}{2} \rho C_D A_F (v_i(t) + v_w(t)) ((v_i(t) + v_w(t)) + 2\tau_i (a_i(t) + \dot{v}_w(t)))}{\tau_i}. \end{aligned} \quad (38)$$

Thus, the nonlinear state feedback chosen for linearizing can be defined by:

$$\begin{aligned} u_i^*(t) &= m_i u_i(t) + g \sin(\theta_i(t)) [1 - \tau_i \mu_R \dot{\theta}_i(t)] \\ &\quad + g \cos(\theta_i(t)) [1 + \tau_i \dot{\theta}_i(t)] \\ &\quad + \frac{1}{2} \rho C_D A_F (v_i(t) + v_w(t)) \\ &\quad ((v_i(t) + v_w(t)) + 2\tau_i (a_i(t) + \dot{v}_w(t))). \end{aligned} \quad (39)$$

Under the new feedback control input, the Equation (4) can be rewritten as:

$$\tau_i \dot{a}_i(t) + a_i(t) = u_i(t). \quad (40)$$

## APPENDIX B. CONNECTION BETWEEN LYAPUNOV-KRASOVSKII STABILITY THEOREM AND SECOND LYAPUNOV METHOD.

First, we present a lemma on the Lyapunov function:

**Lemma 11.** [59]. Let a system  $\dot{x}(t) = f(x(t), x(t-h(t)))$  with  $f(0, 0) = 0$ . Assume the Lyapunov function  $F : G \rightarrow \mathbb{R}$  exists with  $x, y \in G$ ,  $F(y) < F(x)$  implies

$$(\dot{F}(x) f(x, y)) (\dot{F}(x) f(x, y)) \leq 0. \quad (41)$$

Then the solution  $x(t) \equiv 0$  is stable.

Suppose there exists a Lyapunov function  $F : \mathbb{R}^n \rightarrow \mathbb{R}$ . Then define functional  $V : C \rightarrow \mathbb{R}$  as follows:

$$V(\phi) := \max_{-h \leq \theta \leq 0} F(\phi(\theta)), (\forall \phi \in C). \quad (42)$$

By definition, the following conditions hold:

$$\dot{V}(\phi) \begin{cases} \leq 0, & \text{if } F(\phi(0)) < V(\phi), \\ = \max(\dot{F}(\phi(0)), f(\phi(0), \phi(-h(t))), 0), & \text{if } F(\phi(0)) = V(\phi), \end{cases} \quad (43)$$

where  $f(\phi(0), \phi(-h(t))) = \Psi\phi(0) + \Psi_d\phi(-h(t))$ .

Thus  $\dot{V}(\phi) > 0$  holds if and only if the following condition holds:

$$F(\phi(0)) = \max_{-h \leq \theta \leq 0} F(\phi(\theta)) \text{ and } (\dot{F}(\phi(0)), f(\phi(0), \phi(-h(t)))) > 0. \quad (44)$$

The function  $F$  can be defined in some neighborhood  $G \subset \mathbb{R}^n$ . And the functional  $V$  is then defined for  $\phi \in C$  with values in  $G$ .

Suppose Equation (44) holds for some functions  $\phi \in C$ , then we can obtain the inequality  $F(\phi(-h(t))) < F(\phi(0))$  making  $\phi$  arbitrarily small. Thus the second condition in Equation (44) still holds, but conflicts with Lemma 11. Therefore  $\dot{V}(\phi) \leq 0$  holds constantly for all  $\phi$ .

It can be concluded that the Lyapunov-Krasovskii stability theorem can be considered as an extension of the second Lyapunov method to functional space. This extension does not introduce any additional constraints since it only constrains the definite sign at the start and end points instead of in the neighborhood. As a result, the stability conditions obtained using the Lyapunov-Krasovskii stability theorem are more accurate than those obtained using the second Lyapunov method. This conclusion has been supported by previous research [34, 35].

#### APPENDIX C. ATTACHMENTS UPLOADED TO GITHUB

The uploaded code for this paper includes the formulation of Theorem 3 and the construction of LMIs for Theorem 8. Additionally, matrices corresponding to the four sets of control parameters for PLF, as selected in Section V-B, and three sets for PF, BD, and BDL, as selected in Section V-C, which are compatible with Theorem 8, have been included in the repository. The file repository URL is: <https://github.com/ruantiancheng/code-of-paper8>.

#### ACKNOWLEDGMENT

This research was sponsored by the National Key Research and Development Program of China (No. 2022ZD0115600), National Science Foundation of China (No. 52072067), Post-graduate Research & Practice Innovation Program of Jiangsu Province (KYCX22\_0266), and Natural Science Foundation of Jiangsu Province (No. BK20210249).

#### REFERENCES

- [1] D. Schrank, B. Eisele, and T. Lomax, “Urban mobility report 2019,” 2019, publisher: Texas Transportation Institute.
- [2] I. G. Jin and G. Orosz, “Optimal control of connected vehicle systems with communication delay and driver reaction time,” *IEEE Transactions on Intelligent Transportation Systems*, vol. 18, no. 8, pp. 2056–2070, 2016.
- [3] T. Ruan, H. Wang, L. Zhou, Y. Zhang, C. Dong, and Z. Zuo, “Impacts of Information Flow Topology on Traffic Dynamics of CAV-MV Heterogeneous Flow,” *IEEE Transactions on Intelligent Transportation Systems*, pp. 1–16, 2022.
- [4] Z. Zhong, E. E. Lee, M. Nejad, and J. Lee, “Influence of CAV clustering strategies on mixed traffic flow characteristics: An analysis of vehicle trajectory data,” *Transportation Research Part C: Emerging Technologies*, vol. 115, p. 102611, 2020.
- [5] B. van Arem, M. M. Abbas, X. Li, L. Head, X. Zhou, D. Chen, R. Bertini, S. P. Mattingly, H. Wang, and G. Orosz, “Integrated traffic flow models and analysis for automated vehicles,” in *Road Vehicle Automation 3*. Springer, 2016, pp. 249–258.
- [6] L. Ye and T. Yamamoto, “Impact of dedicated lanes for connected and autonomous vehicle on traffic flow throughput,” *Physica A: Statistical Mechanics and its Applications*, vol. 512, pp. 588–597, 2018.
- [7] T. Ruan, L. Zhou, and H. Wang, “Stability of heterogeneous traffic considering impacts of platoon management with multiple time delays,” *Physica A: Statistical Mechanics and its Applications*, vol. 583, p. 126294, 2021.
- [8] R. E. Wilson and J. A. Ward, “Car-following models: Fifty years of linear stability analysis - a mathematical perspective,” *Transportation Planning and Technology*, vol. 34, no. 1, pp. 3–18, 2011.
- [9] R. E. Wilson, “Mechanisms for spatio-temporal pattern formation in highway traffic models,” *Philosophical Transactions of the Royal Society A: Mathematical, Physical and Engineering Sciences*, vol. 366, no. 1872, pp. 2017–2032, 2008, publisher: The Royal Society London.
- [10] B. Goñi-Ros, W. J. Schakel, A. E. Papacharalampous, M. Wang, V. L. Knoop, I. Sakata, B. van Arem, and S. P. Hoogendoorn, “Using advanced adaptive cruise control systems to reduce congestion at sags: An evaluation based on microscopic traffic simulation,” *Transportation Research Part C: Emerging Technologies*, vol. 102, pp. 411–426, 2019, publisher: Elsevier.
- [11] I. K. Nikолос, A. I. Delis, and M. Papageorgiou, “Macroscopic Modelling and Simulation of ACC and CACC Traffic,” in *IEEE Conference on Intelligent Transportation Systems, Proceedings, ITSC*, vol. 2015-Octob. IEEE, 2015, pp. 2129–2134.
- [12] A. Kesting, M. Treiber, and D. Helbing, “Enhanced intelligent driver model to access the impact of driving strategies on traffic capacity,” *Philosophical Transactions of the Royal Society A: Mathematical, Physical and Engineering Sciences*, vol. 368, no. 1928, pp. 4585–4605, 2010, publisher: The Royal Society Publishing.
- [13] F. Navas and V. Milanés, “Mixing V2V- and non-V2V-equipped vehicles in car following,” *Transportation Research Part C: Emerging Technologies*, vol. 108, no. September, pp. 167–181, 2019. [Online]. Available: <https://doi.org/10.1016/j.trc.2019.08.021>
- [14] L. Zhou, T. Ruan, K. Ma, C. Dong, and H. Wang, “Impact of CAV platoon management on traffic flow considering degradation of control mode,” *Physica A: Statistical Mechanics and its Applications*, vol. 581, p. 126193, 2021.
- [15] K. C. Dey, L. Yan, X. Wang, Y. Wang, H. Shen, M. Chowdhury, L. Yu, C. Qiu, and V. Soundararaj, “A review of communication, driver characteristics, and controls aspects of cooperative adaptive cruise control (CACC),” *IEEE Transactions on Intelligent Transportation Systems*, vol. 17, no. 2, pp. 491–509, 2015.
- [16] Y. Zheng, S. E. Li, K. Li, and L.-Y. Wang, “Stability margin improvement of vehicular platoon considering undirected topology and asymmetric control,” *IEEE Transactions on Control Systems Technology*, vol. 24, no. 4, pp. 1253–1265, 2015, publisher: IEEE.
- [17] A. Ghiasi, O. Hussain, Z. S. Qian, and X. Li, “A mixed traffic capacity analysis and lane management model for connected automated vehicles: A Markov chain method,” *Transportation Research Part B: Methodological*, vol. 106, pp. 266–292, 2017.
- [18] Y. Li, Z. Chen, Y. Yin, and S. Peeta, “Deployment of roadside units to overcome connectivity gap in transportation networks with mixed traffic,” *Transportation*

- Research Part C: Emerging Technologies*, vol. 111, pp. 496–512, 2020, publisher: Elsevier.
- [19] M. Sala and F. Soriguera, “Capacity of a freeway lane with platoons of autonomous vehicles mixed with regular traffic,” *Transportation research part B: methodological*, vol. 147, pp. 116–131, 2021, publisher: Elsevier.
- [20] X. Chang, H. Li, J. Rong, and X. Zhao, “Analysis on traffic stability and capacity for mixed traffic flow with platoons of intelligent connected vehicles,” *Physica A: Statistical Mechanics and its Applications*, vol. 557, p. 124829, 2020.
- [21] Y. Zhou, M. Wang, and S. Ahn, “Distributed model predictive control approach for cooperative car-following with guaranteed local and string stability,” *Transportation research part B: methodological*, vol. 128, pp. 69–86, 2019.
- [22] M. Montanino and V. Punzo, “On string stability of a mixed and heterogeneous traffic flow: A unifying modelling framework,” *Transportation Research Part B: Methodological*, vol. 144, pp. 133–154, 2021.
- [23] W. Yu, X. Hua, and W. Wang, “Investigating the longitudinal impact of cooperative adaptive cruise control vehicle degradation under communication interruption,” *IEEE Intelligent Transportation Systems Magazine*, 2021.
- [24] H. Liu, X. Kan, S. E. Shladover, X.-Y. Lu, and R. E. Ferlis, “Impact of cooperative adaptive cruise control on multilane freeway merge capacity,” *Journal of Intelligent Transportation Systems*, vol. 22, no. 3, pp. 263–275, 2018.
- [25] L. Xiao, M. Wang, W. Schakel, and B. van Arem, “Unravelling effects of cooperative adaptive cruise control deactivation on traffic flow characteristics at merging bottlenecks,” *Transportation research part C: emerging technologies*, vol. 96, pp. 380–397, 2018.
- [26] R. Herman, E. W. Montroll, R. B. Potts, and R. W. Rothery, “Traffic dynamics: analysis of stability in car following,” *Operations research*, vol. 7, no. 1, pp. 86–106, 1959.
- [27] X. Zhang and D. F. Jarrett, “Stability analysis of the classical car-following model,” *Transportation Research Part B: Methodological*, vol. 31, no. 6, pp. 441–462, 1997.
- [28] Y. Li, D. Sun, and M. Cui, “Lyapunov stability analysis for the full velocity difference car-following model,” *Control Theory & Applications*, vol. 12, p. 014, 2010.
- [29] Y. Li, H. Zhu, M. Cen, Y. Li, R. Li, and D. Sun, “On the stability analysis of microscopic traffic car-following model: a case study,” *Nonlinear Dynamics*, vol. 74, no. 1, pp. 335–343, 2013.
- [30] G. K. Kamath, K. Jagannathan, and G. Raina, “Car-following models with delayed feedback: local stability and hopf bifurcation,” in *2015 53rd Annual Allerton Conference on Communication, Control, and Computing (Allerton)*. IEEE, 2015, pp. 538–545.
- [31] J. Sun, Z. Zheng, and J. Sun, “Stability analysis methods and their applicability to car-following models in conventional and connected environments,” *Transportation research part B: methodological*, vol. 109, pp. 212–237, 2018, publisher: Elsevier.
- [32] H. Lhachemi and C. Prieur, “Feedback stabilization of a class of diagonal infinite-dimensional systems with delay boundary control,” *IEEE Transactions on Automatic Control*, vol. 66, no. 1, pp. 105–120, 2020.
- [33] E. Fridman, “Descriptor discretized lyapunov functional method: analysis and design,” *IEEE Transactions on Automatic control*, vol. 51, no. 5, pp. 890–897, 2006.
- [34] Y. Wang, Y. Xia, and P. Zhou, “Fuzzy-model-based sampled-data control of chaotic systems: A fuzzy time-dependent lyapunov–krasovskii functional approach,” *IEEE Transactions on fuzzy systems*, vol. 25, no. 6, pp. 1672–1684, 2016.
- [35] H.-H. Lian, S.-P. Xiao, H. Yan, F. Yang, and H.-B. Zeng, “Dissipativity analysis for neural networks with time-varying delays via a delay-product-type lyapunov functional approach,” *IEEE transactions on neural networks and learning systems*, vol. 32, no. 3, pp. 975–984, 2020.
- [36] A. A. Martyniuk and R. Gutovski, “Integral inequalities and stability of motion,” *Kiev Izdatel Naukova Dumka*, 1979.
- [37] C.-K. Zhang, Y. He, L. Jiang, M. Wu, and H.-B. Zeng, “Stability analysis of systems with time-varying delay via relaxed integral inequalities,” *Systems & Control Letters*, vol. 92, pp. 52–61, 2016, publisher: Elsevier.
- [38] D. Li, Q. Liu, and X. Ju, “Uniform decay estimates for solutions of a class of retarded integral inequalities,” *Journal of Differential Equations*, vol. 271, pp. 1–38, 2021, publisher: Elsevier.
- [39] S. Saravanan, M. Syed Ali, G. Rajchakit, B. Hamachukiattikul, B. Priya, and G. K. Thakur, “Finite-time stability analysis of switched genetic regulatory networks with time-varying delays via Wirtinger’s integral inequality,” *Complexity*, vol. 2021, 2021, publisher: Hindawi.
- [40] R. Suresh and A. Manivannan, “Robust stability analysis of delayed stochastic neural networks via Wirtinger-based integral inequality,” *Neural Computation*, vol. 33, no. 1, pp. 227–243, 2021, publisher: MIT Press One Rogers Street, Cambridge, MA 02142-1209, USA journals-info ....
- [41] M. Park, O. Kwon, J. H. Park, S. Lee, and E. Cha, “Stability of time-delay systems via Wirtinger-based double integral inequality,” *Automatica*, vol. 55, pp. 204–208, 2015, publisher: Elsevier.
- [42] K. Gu, J. Chen, and V. L. Kharitonov, *Stability of time-delay systems*. Springer Science & Business Media, 2003.
- [43] P. Park, J. W. Ko, and C. Jeong, “Reciprocally convex approach to stability of systems with time-varying delays,” *Automatica*, vol. 47, no. 1, pp. 235–238, 2011, publisher: Elsevier.
- [44] P. POPEO, “Federal communications commission,” 2020.
- [45] L. L. C. Verizon North, “Federal Communications Commission,” *Proceeding Number*, vol. 19, p. 354, 2020.
- [46] M. Wang, “Infrastructure assisted adaptive driving to stabilise heterogeneous vehicle strings,” *Transportation Research Part C: Emerging Technologies*, vol. 91, no. April 2017, pp. 276–295, 2018, publisher: Elsevier. [On-

- line]. Available: <https://doi.org/10.1016/j.trc.2018.04.010>
- [47] D. Jia and D. Ngoduy, “Enhanced cooperative car-following traffic model with the combination of V2V and V2I communication,” *Transportation Research Part B: Methodological*, vol. 90, pp. 172–191, 2016, publisher: Elsevier.
- [48] V. Vukadinovic, K. Bakowski, P. Marsch, I. D. Garcia, H. Xu, M. Sybis, P. Sroka, K. Wesolowski, D. Lister, and I. Thibault, “3GPP C-V2X and IEEE 802.11p for Vehicle-to-Vehicle communications in highway platooning scenarios,” *Ad Hoc Networks*, vol. 74, pp. 17–29, 2018.
- [49] H. V. Vu, Z. Liu, D. H. N. Nguyen, R. Morawski, and T. Le-Ngoc, “Multi-agent reinforcement learning for joint channel assignment and power allocation in platoon-based C-V2X systems,” *arXiv preprint arXiv:2011.04555*, 2020.
- [50] D. Martín-Sacristán, S. Roger, D. Garcia-Roger, J. F. Monserrat, P. Spapis, C. Zhou, and A. Kaloxylos, “Low-Latency Infrastructure-Based Cellular V2V Communications for Multi-Operator Environments With Regional Split,” *IEEE Transactions on Intelligent Transportation Systems*, vol. 22, no. 2, pp. 1052–1067, 2020.
- [51] M. Pirani, S. Baldi, and K. H. Johansson, “Impact of Network Topology on the Resilience of Vehicle Platoons,” *IEEE Transactions on Intelligent Transportation Systems*, 2022.
- [52] K. Gu and Y. Liu, “Lyapunov–Krasovskii functional for uniform stability of coupled differential-functional equations,” *Automatica*, vol. 45, no. 3, pp. 798–804, 2009.
- [53] P. Pepe and Z.-P. Jiang, “A Lyapunov–Krasovskii methodology for ISS and iISS of time-delay systems,” *Systems & Control Letters*, vol. 55, no. 12, pp. 1006–1014, 2006, publisher: Elsevier.
- [54] M. Wang, S. P. Hoogendoorn, W. Daamen, B. van Arem, B. Shyrokau, and R. Happee, “Delay-compensating strategy to enhance string stability of adaptive cruise controlled vehicles,” *Transportmetrica B*, vol. 6, no. 3, pp. 211–229, 2018. [Online]. Available: <https://doi.org/10.1080/21680566.2016.1266973>
- [55] Y. Zhou, S. Ahn, M. Wang, and S. Hoogendoorn, “Stabilizing mixed vehicular platoons with connected automated vehicles: An H-infinity approach,” *Transportation Research Part B: Methodological*, vol. 132, pp. 152–170, 2020.
- [56] C. Fu and T. Sayed, “Comparison of threshold determination methods for the deceleration rate to avoid a crash (drac)-based crash estimation,” *Accident Analysis & Prevention*, vol. 153, p. 106051, 2021.
- [57] ——, “Random parameters bayesian hierarchical modeling of traffic conflict extremes for crash estimation,” *Accident Analysis & Prevention*, vol. 157, p. 106159, 2021.
- [58] Y. Zheng, S. E. Li, J. Wang, D. Cao, and K. Li, “Stability and scalability of homogeneous vehicular platoon: Study on the influence of information flow topologies,” *IEEE Transactions on intelligent transportation systems*, vol. 17, no. 1, pp. 14–26, 2015.
- [59] V. Kolmanovskii and A. Myshkis, *Introduction to the Theory and Applications of Functional Differential Equations*. Dordrecht: Springer Netherlands, 1999.